Evaluation of Material Models within LS-DYNA® for a Kevlar/Epoxy Composite Honeycomb

Michael Polanco
ATK Space Systems
Hampton, Virginia 23681
michael.a.polanco@nasa.gov

Sotiris Kellas and Karen Jackson
NASA Langley Research Center
Hampton, Virginia 23681
sotiris.kellas-1@nasa.gov
karen.e.jackson-1@nasa.gov

Abstract

The performance of material models to simulate a novel composite honeycomb Deployable Energy Absorber (DEA) was evaluated using the nonlinear explicit dynamic finite element code LS-DYNA®. Prototypes of the DEA concept were manufactured using a Kevlar/Epoxy composite material in which the fibers are oriented at ±45º with respect to the loading axis. The development of the DEA has included laboratory tests at subcomponent and component levels such as three-point bend testing of single hexagonal cells, dynamic crush testing of single multi-cell components, and impact testing of a full-scale fuselage section fitted with a system of DEA components onto multi-terrain environments. Due to the thin nature of the cell walls, the DEA was modeled using shell elements. In an attempt to simulate the dynamic response of the DEA, it was first represented using *MAT_LAMINATED_COMPOSITE_FABRIC, or *MAT_58, in LS-DYNA. Values for each parameter within the material model were generated such that an in-plane isotropic configuration for the DEA material was assumed. Analytical predictions showed that the load-deflection behavior of a single-cell during three-point bending was within the range of test data, but predicted the DEA crush response to be very stiff. In addition, a *MAT_PIECEWISE_LINEAR_PLASTICITY, or *MAT_24, material model in LS-DYNA was developed, which represented the Kevlar/Epoxy composite as an isotropic elastic-plastic material with input from ±45º tensile coupon data. The predicted crush response matched that of the test and localized folding patterns of the DEA were captured under compression, but the model failed to predict the single-cell three-point bending response.

Introduction

NASA's Subsonic Rotary Wing aeronautics program is evaluating a novel Deployable Energy Absorbing (DEA) [1, 2] concept for improved rotorcraft crashworthiness. The DEA is a composite honeycomb cellular structure with flexible hinged walls that can be externally deployed omnidirectionally to provide energy dissipation. Once expanded, the DEA becomes an efficient cellular structure, possessing high strength and stiffness along the cell axis compared to the transverse direction. The cell walls in the DEA are made of a single woven ply of 0.01-in thick Kevlar-129 fabric impregnated with RenInfusion 8601 epoxy resin. The fibers in each composite ply are oriented at ±45º with respect to the loading direction. The DEA has been considered for impact energy application in rotorcraft, where the energy absorbers would be deployed in the event of an emergency landing.

Several static and dynamic tests were conducted to characterize the Kevlar/Epoxy composite material for the DEA, as described in [1]. These included three-point bending of single hexagonal cells, vertical dynamic crushing of single DEA components, and multi-terrain impact tests of DEA blocks fitted under a composite fuselage section. The mechanical behavior of the honeycomb needed to be fully understood to guide future studies of the DEA for impact attenuation in full-scale helicopter crashes. Consequently, small single-cell specimens were studied before addressing multi-cell components. Shell-based finite element models of these tests were created and executed using LS-DYNA®* [3]. The use of

---

shell elements in modeling the composite honeycomb provides for a more realistic and accurate representation of the DEA geometry, rather than by using solid elements. In addition, property diminishment of individual plies can be implemented based on damage mechanics models [4]. Success in simulating the crush response of the DEA is highly dependent on accurately modeling the cell wall material and geometry. The modeling of composites has long been complicated by the failure modes they exhibit under compression, such as local buckling, delamination, and tearing [4]. These interactive failure modes often complicate the ability to model the material crush response of the DEA under load. This paper will describe the work to efficiently simulate the buckling and folding associated with the DEA response. This work includes test/analysis correlation of single hexagonal cells under transverse loading, crushing of multi-cell DEA components, and the crush response of a full-scale fuselage section fitted with a system of DEAs.

Descriptions of Applied LS-DYNA Material Models for Kevlar/Epoxy

To accurately characterize Kevlar/Epoxy, an LS-DYNA material model was needed with the capability to predict the observed failure mechanisms in the DEA. The model would also need to demonstrate good functionality with the use of a shell configuration, which is used to best capture the geometry of the DEA. Two material models in LS-DYNA were considered, and are presented.

Composite Laminate Material Model

The first LS-DYNA material model used to represent the Kevlar/Epoxy composite was *MAT_LAMINATED_COMPOSITE_FABRIC, or *MAT_58. The *MAT_58 material model was initially chosen as a result of past success in predicting the impact damage of the Reinforced Carbon-Carbon leading edge panels of the Space Shuttle Columbia [5]. *MAT_58 is a continuum damage mechanics material model based on the Matzenmiller-Lubliner-Taylor model [6] designed for use with shell elements to simulate composite laminates and woven fabrics. The model requires input of material properties in shear, tension, and compression to define stress-strain behavior within the laminate. The user specifies in-plane elastic moduli and Poisson's ratio in three planes. The maximum strength in tension, compression, and shear is also specified at corresponding strain values. A representation of the stress-strain curve for shear is illustrated in Figure 1. The first slightly nonlinear portion of the stress-strain curve for shear loading must be specified, which occurs at a shear strain Gamma1 and a shear stress Tau1. The maximum shear strength SC occurs at a shear strain specified as GMS in the model. After the maximum shear strength SC is reached, the strength is multiplied by the factor SLIMS which can range from 0 to 1. The stress-limiting factors SLIMT, SLIMC, and SLIMS control the material's behavior past its "strength" in tension, compression, and shear, respectively. The material is modeled as perfectly plastic after this point. The stress after maximum strength is held constant until elements reach a strain specified by the ERODS parameter in the material model, where the elements are then deleted and removed from the solution. Additional information on this material model can be found in Reference 3.
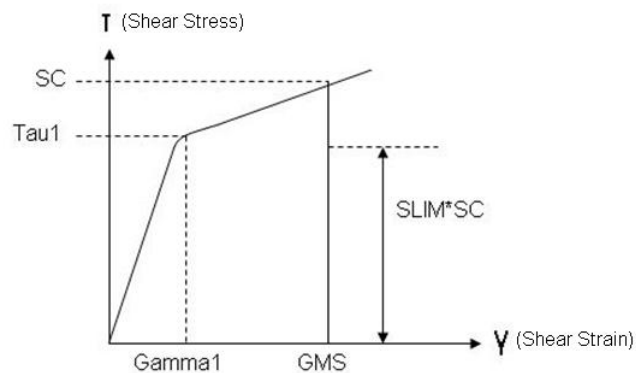

Figure 1. Shear stress-strain curve used for material within *MAT_58 [3].

The input parameters for *MAT_58 were determined based on data obtained from five tensile tests conducted on single-ply fabric Kevlar/Epoxy coupons oriented with weave at 0°/90° and ±45° with respect to the loading axis. All coupons had a nominal thickness value of 0.01 inches. Tensile properties for the model were obtained from 0°/90° tensile data while shear properties were obtained from ±45° tensile coupon tests. The ±45° coupons were pulled at 1 inch per minute (ipm) and 20 ipm to assess any effects of strain rates on the stress-strain response. Different strain rates were not considered for the 0°/90° coupons since the material tensile response is not affected by strain rate for this orientation. The average results from both tensile tests can be found in Figure 2.

(a) Average 0°/90° degree tensile test results   (b) Average ±45° tensile test results
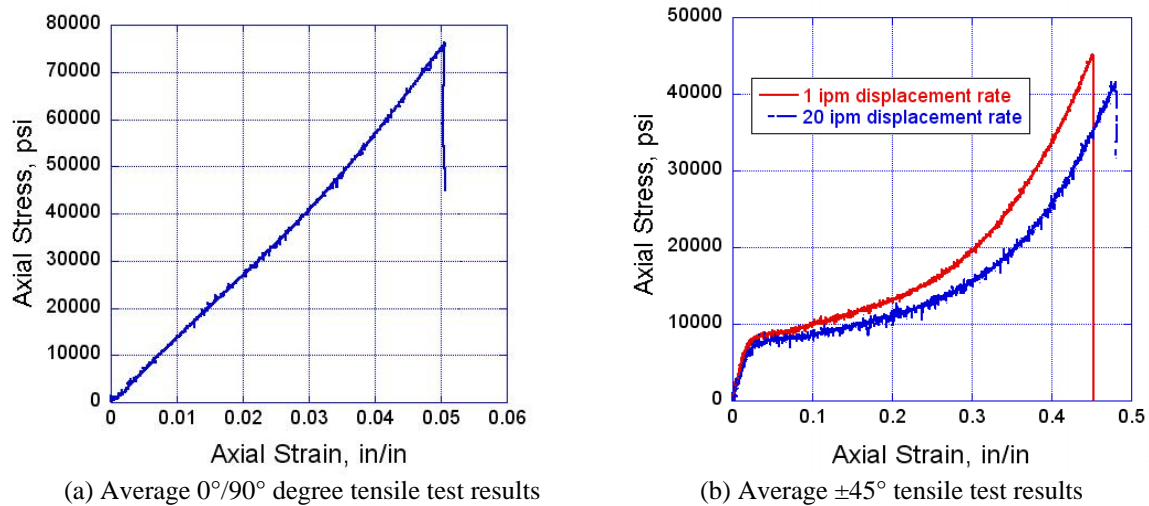
Figure 2. Stress-strain curves for 0°/90° and ±45° coupons.

Negligible differences in the elastic responses of the ±45° tensile coupons were observed based on the strain rates considered during testing. However, the response deviated afterwards, with the ultimate strengths differing by about 8%, and a 6.25% difference in ultimate strain. The stress-strain plot for the ±45° configuration shows a sudden rise in stress before material failure. This effect is attributed to scissoring of the fibers, or the tendency of the fibers to align with the load direction, and a reduction in the cross-sectional area. Because the specimen thickness was small, it was difficult to obtain compression properties. Consequently, the compression properties were assumed to be equal to those in tension. Initial *MAT_58 properties based on these tests can be found in [1].

Piecewise Linear Plasticity Material Model

As will be shown later, the difficulty of characterizing Kevlar/Epoxy using a composite material model in LS-DYNA drove a decision to use a second model that was much less complex than *MAT_58. The second LS-DYNA material model considered for Kevlar/Epoxy was *MAT_PIECEWISE_LINEAR_PLASTICITY, otherwise known as *MAT_24. In the model, the user must specify the elastic modulus, Poisson's ratio, and yield stress of the material. The user must also define an arbitrary effective-stress versus effective plastic strain curve to be used in the isotropic material model. Input properties for the *MAT_24 model were taken from the 20 ipm stress-strain curve, shown in Figure 2b, and are listed in Table 1. The curve generated from a higher strain rate was used since the material model application will involve high strain rates. The plastic portion of the curve was utilized in conjunction with the ±45° fiber orientation of the Kevlar cell walls in the DEA, and the assumption was made that the tensile response was equivalent to the compressive response.

Table 1. Property values used in *MAT_24

Parameter No	Symbol	Parameter values
1	E (psi)	340000
2	PRBA	0.3
3	SIGY (psi)	7500
4	ETAN (psi)	0

Computer Simulation of Quasi-static Three-Point Bend tests

Efforts to characterize Kevlar/Epoxy began with simulating quasi-static bending of a single hexagonal cell representing the geometry of the DEA cells. The original intention of these tests was to understand the shear stability of the cells. Tests performed on the single-cells, described in [1], served as the basis for setting up the finite element models. Preliminary work on developing a shell-based model for the DEA was presented in Reference 1, which included results from LS-DYNA models for three-point bending of a single hexagonal cell. The work presented here is a continuation of those modeling efforts. A representation of an LS-DYNA single-cell model can be seen in Figure 3 for a 1.0-inch cell width. The general setup described in Reference 1 for the single-cell model was kept intact. *SECTION_SHELL cards were used with *MAT_58 to specify both the thickness of the Kevlar/Epoxy and the direction of the fibers at ±45° from the loading axis. An *INTEGRATION_SHELL card was also used to define four integration points through the thickness. The reactive forces to the applied quasi-static load were measured using the *BOUNDARY_SPC_SET card, which were plotted against transverse displacement of the single-cell. This approach was a more accurate method of obtaining load-displacement data from the single-cell models, since this was how test data was acquired, than the method presented in Reference 1. The model for the single-cell case W=1.0-inch had 27,098 nodes and 25,600 elements, including 13,600 Belytschko-Tsay quadrilateral elements representing the Kevlar/Epoxy cell walls, and 12,000 hexagonal solid elements representing the three Bakelite inserts.

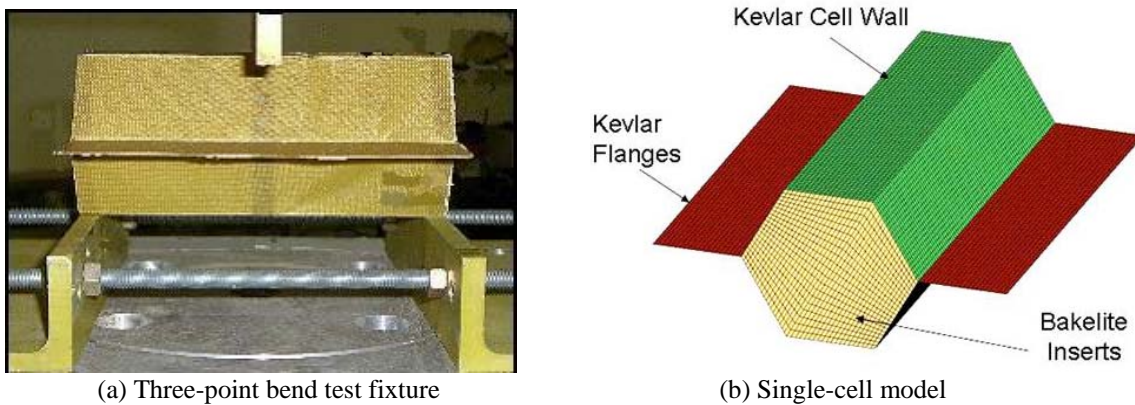(a) Three-point bend test fixture   (b) Single-cell model

Figure 3. Photo and image of single-cell test specimen and model.

The parameter set originally used in *MAT_58 resulted in early failure of the cell wall and a sudden drop in load compared with the test [1]. Hence, to obtain results from LS-DYNA that would accurately characterize the Kevlar/Epoxy composite in three-point bending, a set of parameters was needed for calibration within *MAT_58 which would reconcile the test results with those from LS-DYNA. A Response Surface Methodology (RSM) conducted by Horta [7] was utilized which assessed the influence of each parameter in the material model on the three-point bend response of a single-cell. New parameter sets were generated through multiple LS-DYNA runs to obtain convergence of a load-displacement response derived from parameter values in *MAT_58 using RSM. A total of nine parameter sets for *MAT_58 were derived using RSM and used as input to the model. None of them were able to predict the load-displacement response within a range of 0 to 0.15 inches.
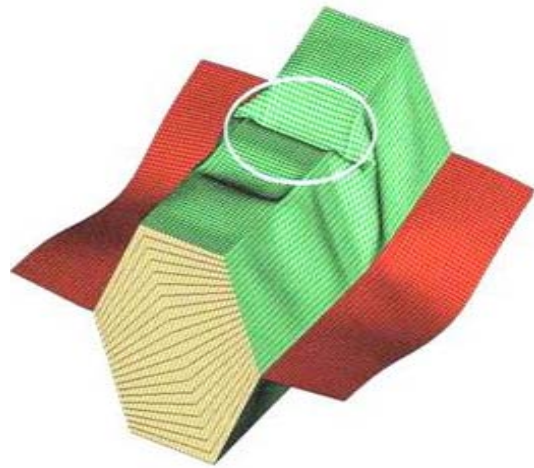
Finally, a new parameter set was created for *MAT_58 by averaging the 9 RSM sets used previously (see Table 2). The best test/analysis correlation was obtained when these average property values were used, as shown in Figure 4a. As shown in the graph, a sudden drop in sustained load occurred at a transverse displacement of 0.08 inches, which made test/analysis correlation difficult past this value for all simulations. The load drops are attributed to global buckling of the fabric for all four geometric cases that were considered [1]. A picture of a buckled single-cell model is found in Figure 4b. Typically, the model solutions required slightly over 5 hours to execute 0.1 seconds of a simulation time on a single PC computer processor. Execution of the model took place using LS-DYNA version 971 with double precision.

Table 2. *MAT_58 property values resulting in best test/analysis correlation for three-point bend simulations. These values were average values from the 9 RMS sets.

Parameter No	Symbol	Average values
1	EA=EB=EC (psi)	1.318e6
2	PRBA	0.3427
3	TAU1 (psi)	5602.8
4	GAMMA1 (psi)	0.0206
5	GAB=GBC=GCA (psi)	153,044.0
6	SLIMT1	0.8152
7	SLIMC1	0.7492
8	SLIMT2	0.6102
9	SLIMC2	0.7724
10	SLIMS	0.3263
11	ERODS	8.0
12	E11C = E22C	0.0508
13	E11T = E22T	0.0471
14	GMS	0.1085
15	XC = YC (psi)	63,750.0
16	XT = YT (psi)	72,454.0
17	SC (psi)	12,560.0
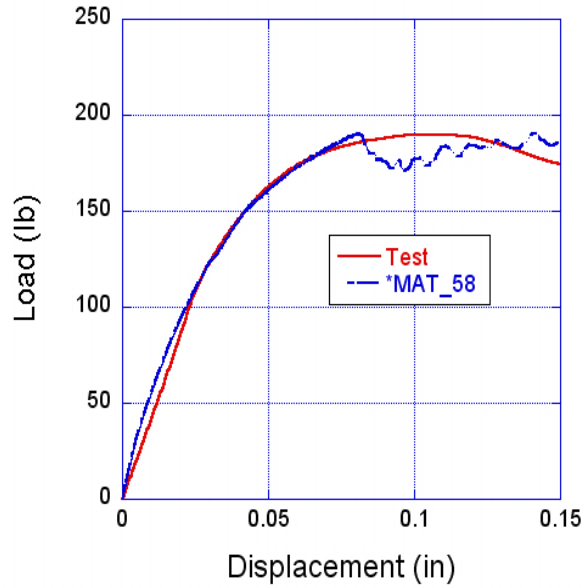
(a) LS-DYNA model results correlated with   (b) Typical global buckling mode shape.
average test data from Table 2.

Figure 4. Test/analysis correlation results, and typical buckling failure in simulation.

Simulating the deformation of the cell wall material and obtaining a curve that gave good correlation with test data presented a challenge for a number of reasons. Manufacturing irregularities were present in each of the test specimens, which could affect the behavior of the fabric under three-point loading. These defects also explain the range of scatter in the test data. As a result, the single-cell models needed to be corrected to account for manufacturing irregularities such as adhesive thickness and filleting variations. For example, a separate model was created, which included extra solid elements near the region of applied loading, to represent fillets created by excess adhesive that could hinder deformation of the fabric near the center Bakelite insert, as shown in Figure 5a. The LS-DYNA results, in comparison with average test data, are shown in Figure 5b.

In addition, the thicknesses of existing test specimens had slight variations from the modeled thicknesses of 0.01 inches for the cell wall and 0.02 inches for the flanges due to the adhesive. As a result, additional LS-DYNA models were created to adjust the thicknesses of the cell wall and flanges within the *SECTION_SHELL card in LS-DYNA. A comparison for these cases is shown in Figure 5c where the flange thickness was increased to 0.025 inches from 0.02 inches to account for the adhesive layer between the flange plies. Incorporating both changes to the model did little to improve correlation with average test data.
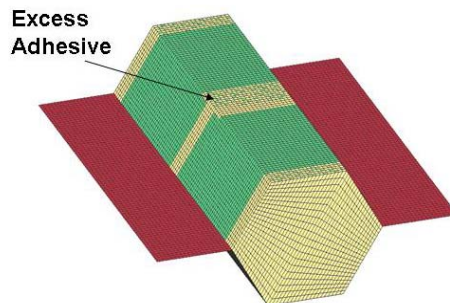
(a) Picture of extra hex elements used
to model adhesive in load region

6

(b) LS-DYNA analysis using extra
hex elements correlated with
average test data

(c) Test/analysis correlation illustrating
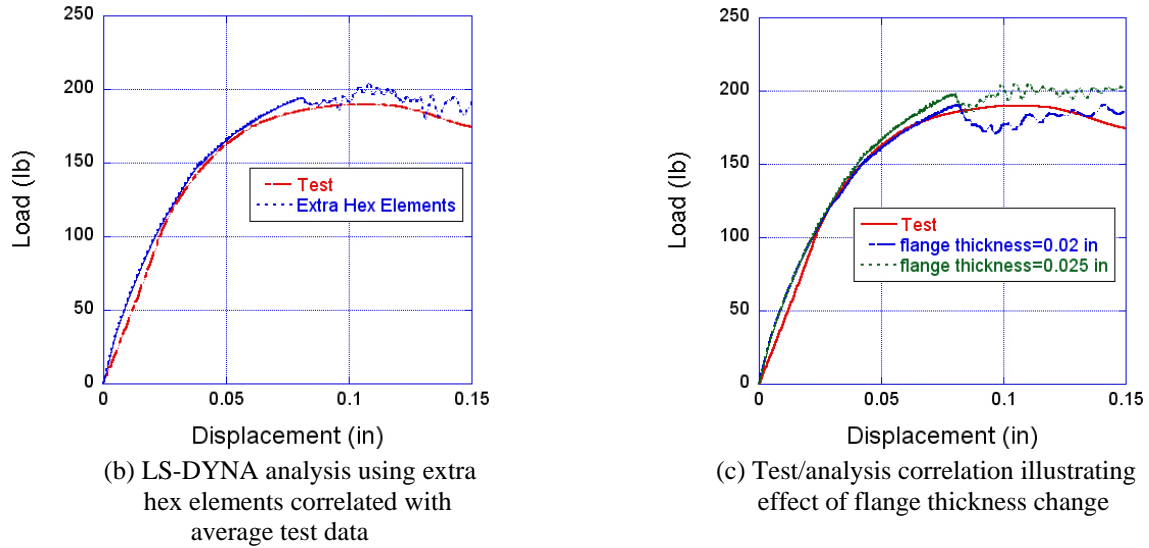effect of flange thickness change

Figure 5. Model with manufacturing irregularities and test/analysis correlation showing their effects.

The *MAT_24 material model was substituted into an existing single-cell model for W=1-inch in place of *MAT_58. As a reminder, the *MAT_24 model is based on the tensile stress-strain response of the ±45° Kevlar/Epoxy coupons. The boundary conditions described previously for the single-cell models remained in place here. The angle layup within *SECTION_SHELL was removed since the model did not assume definition of a composite, but the *INTEGRATION_SHELL cards, setup for *MAT_58, remained intact. Use of this material model led to softer behavior of the three-point bend response due to a lower input Young's modulus and yield stress value; a reason why higher loads were not sustained within the modeled structure. A comparison of the structural response using the two material models can be found in Figure 6.

Although *MAT_24 performed poorly in correlating with the experimental three-point bend data, it was evaluated further for studying the dynamic crush response of the DEA due to the compressive-dominated nature of the test.
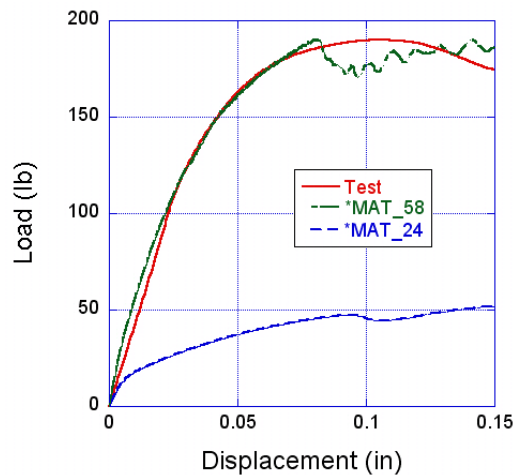

Figure 6. Test/analysis correlation using *MAT_58 and *MAT_24 models in LS-DYNA.

7

Computer Simulations of Multi-Cell DEA Components under Dynamic Crush Loading

Dynamic crush tests of multi-cell honeycomb components were simulated using *MAT_58 and *MAT_24 in LS-DYNA to represent the Kevlar/Epoxy cell walls. Tests that were simulated included DEA components containing 59 and 104 cells, both of whose cells were oriented along the load direction, and a DEA component containing 68 cells, all of which were inclined at 27° with respect to the load axis to study the effect of off-axis crush loading. The finite element models of these DEA components are shown in Figure 7. All models consisted of four parts, including an impact block used to crush the DEA, a reaction surface placed under the honeycomb, one part for plies within the DEA having a 0.01-inch thickness, highlighted in blue, and another part defined for plies with a 0.02-inch thickness, highlighted in green. Like the single-cell models, the use of the *SECTION_SHELL and *INTEGRATION_SHELL cards were used with *MAT_58 to model the composite cell walls. The velocity of the impact block was prescribed using the *INITIAL_VELOCITY_GENERATION card in LS-DYNA.

All finite element models were setup so that the boundary conditions and geometry of the impact block and the honeycomb components were close to those of the test [1]. The reaction surface was constrained using the *BOUNDARY_SPC_SET for all nodes on the surface. The reaction surface and impact block were both modeled as *MAT_RIGID in LS-DYNA. The quad mesh size used on all DEA components was 0.1 inches. Using *MAT_58, the model for the 59-cell component contained 359,195 nodes and 340,778 elements including 127,028 Belytschko-Tsay elements and 213,750 rigid elements that were bypassed in element processing. The model solution required slightly over 40 hours to generate 0.06 seconds of a simulation on four Linux-based processors. The 104-cell component model contained 731,649 nodes, 391,892 Belytschko-Tsay elements, and 318,750 rigid elements. The model solution required approximately 60 hours to simulate 0.06 seconds on four Linux-based processors. The 68-cell off-axis component model contained 435,836 nodes, 171,212 Belytschko-Tsay elements, and 244,800 rigid elements. The model solution required about 34 hours to generate 0.06 seconds of a simulation on four Linux-based processors. As a result of using the *MAT_58 configuration with the parameter values listed in Table 2, the acceleration time histories in Figure 8 show the crush responses of the DEA components to be inherently stiffer than indicated by test data, and little stroke of the DEA was predicted in the simulations. In contrast, during the test, the 59- and 68-cell DEA components crushed to approximately 90% of their original height.
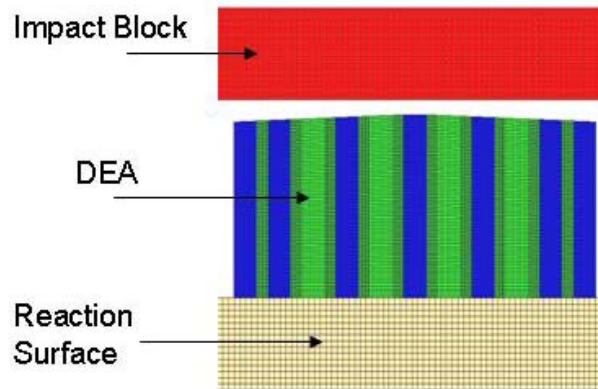

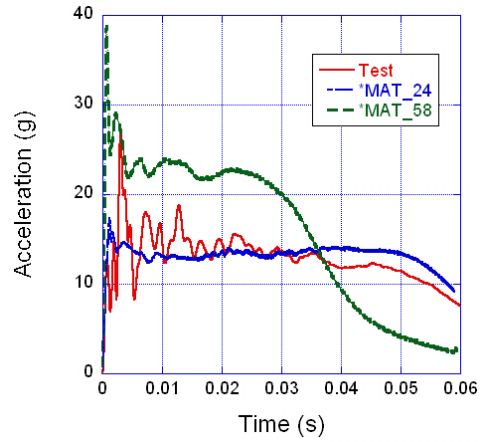(a) 59-cell DEA component
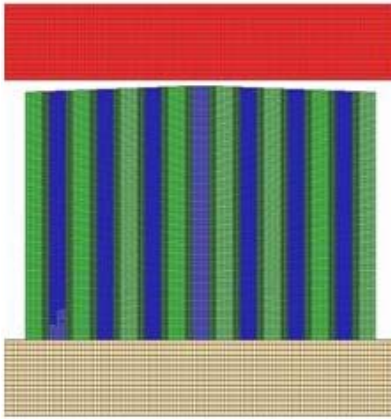
(b) 104-cell DEA component
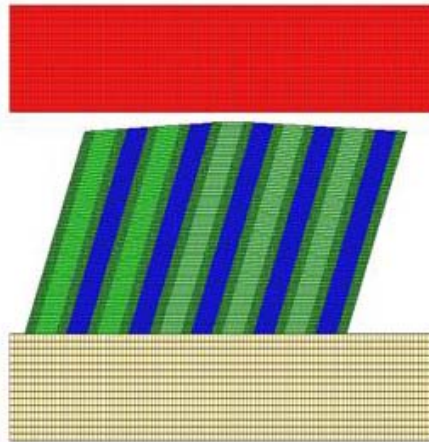
(c) 68-cell DEA component, 27° off-axis

Figure 7. DEA component models with differing geometries

The *MAT_24 material model was used in the existing finite element models of multi-cell DEA components under vertical impact. The boundary conditions prescribed for all models during use of *MAT_58 remained the same. The angle layup definition used for *MAT_58 in *SECTION_SHELL was again removed from use in *MAT_24, and four integration points were used for all shell elements. The 59-cell model solution required 28.4 hours to simulate 0.06 seconds of impact with a nominal edge length of 0.05 inches. The 68-cell model solution required 7.5 hours, while the 104-cell model terminated at 12.5 hours. Both models had a 0.1-inch mesh, and also had termination times of 0.06 seconds. All three models ran on four Linux-based processors. The acceleration time histories shown in Figure 8 indicate that *MAT_24 does a better job in predicting the crush response of the DEA components than *MAT_58. The second acceleration spike seen in the 59-cell DEA component was captured, although not to full magnitude. However, the magnitude of the second acceleration peak, which represents full compaction of the DEA, was over-predicted by a factor of 1.5 in the 68-cell off-axis component and occurred sooner than in the test. The DEA deformation patterns captured for both material models are shown in Figure 9 in comparison with the test specimen. The results indicate that *MAT_24 captures the crushing of the honeycomb better than *MAT_58.
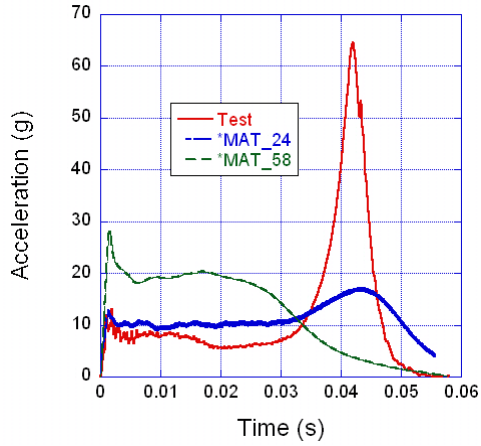
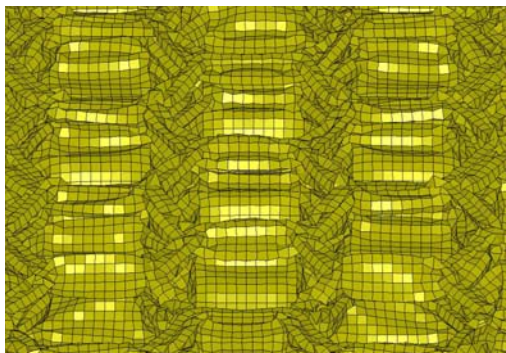(a) 59-cell DEA acceleration-time response

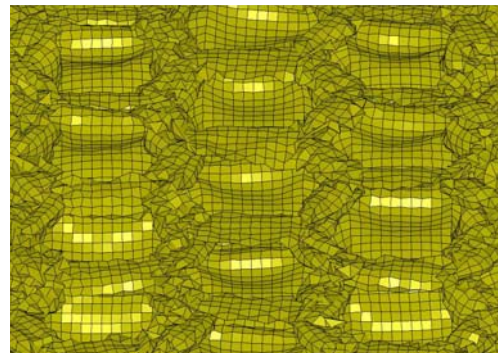(b) 104-cell DEA acceleration-time response
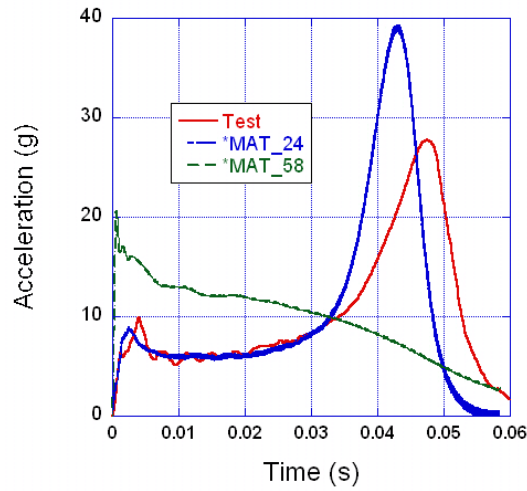
(c) 68-cell DEA acceleration-time response

Figure 8. Test/analysis correlation and comparison between two material models

(a) DEA crush patterns using *MAT_24

(b) DEA crush patterns using *MAT_58

10

(c) DEA component post-test

Figure 9. Test/simulation comparisons of DEA crush using *MAT_24 and *MAT_58.

Fuselage Section with DEA Impact into Concrete

LS-DYNA models were developed to simulate multi-terrain impacts of a composite fuselage section fitted with the DEA. Two different impact surfaces were considered during this study: concrete and soft soil (sifted sand). A picture of the test article is found in Figure 10a. The conditions employed in both finite element models were based on the impact tests described in Reference 8. The model for impact onto concrete contained 13 parts; 126,500 nodes and 144,747 elements including 129,573 Belytschko-Tsay quadrilateral shell elements, 188 beam elements, 40 mass elements, and 14,946 hexagonal solid elements. The shell elements in the model represented the inner and outer skins of the composite fuselage, the concrete that served as the impact surface, and the DEA components. The solid elements represented the upper-cabin foam core and the floor foam core. Concrete was modeled using the *MAT_RIGID property in LS-DYNA. The inner and outer skins of the fuselage were modeled using *MAT_PLASTIC_KINEMATIC to account for kinematic hardening plasticity in the material, and the DEA components were modeled using *MAT_24 with four integration points through the thickness. The fuselage section model was the same as described in Reference 1.

Contact problems related to the hourglass formulations for shells in LS-DYNA led to instability within the *MAT_58 material model and these issues have not been resolved. Thus, results are not presented here using *MAT_58. All solid elements were modeled as linear elastic using *MAT_ELASTIC in LS-DYNA. The beam elements in the model represented the seat tracks that were mounted to the floor of the fuselage. The mass elements represented the ten 100-lb lead masses attached to the seat tracks. Four shell DEA components were attached to the fuselage model using the *TIED_SHELL_EDGE_TO_SURFACE option in LS-DYNA. A *CONTACT_AUTOMATIC_SINGLE_SURFACE algorithm was used to define contact interfaces between the concrete surface and the DEA in addition to modeling self-contact within element segments of the DEA. The nodes on the concrete impact surface, represented by shell elements, were fixed in the model. A mesh size of 0.5 inches was used on all four DEA components. An impact velocity of 38.4 fps was prescribed onto the fuselage through the *INITIAL_VELOCITY_GENERATION card in LS-DYNA. A perfectly vertical orientation of the fuselage was assumed in the model. The model required 4.5 hours to run on four Linux-based processors. An image of the model is shown in Figure 10. On average, the simulation predicted about 13.7 inches of DEA crush, compared to 14.5 inches of average measured crush during the test. Acceleration time history results, shown in Figure 11, were taken from the front left, center left, center right, and rear right lead blocks on the floor of the fuselage. All LS-DYNA results were filtered using an SAE low-pass filter at a 60 Hz cutoff frequency.
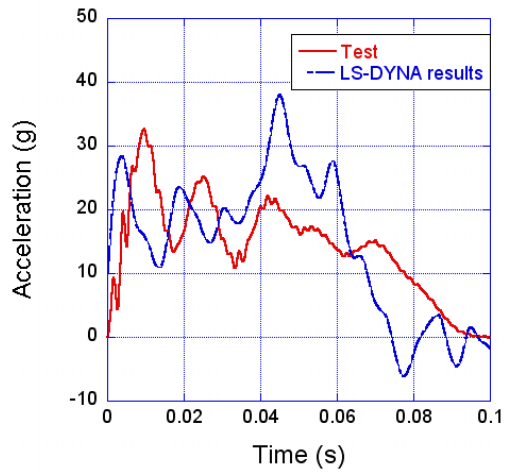
(a) Test article with accelerometer location labels taken for analysis correlation.
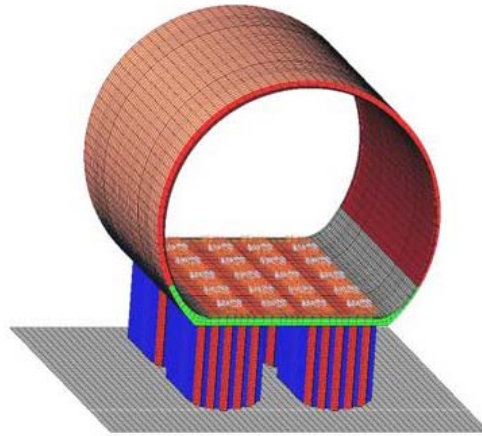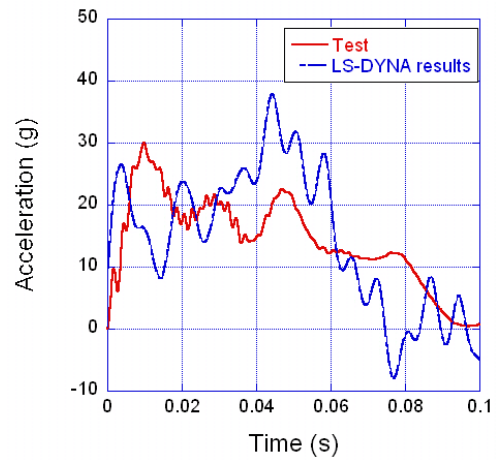

(b) Finite Element Model of Fuselage w/DEA

Figure 10. Composite fuselage section with DEA impacting concrete.

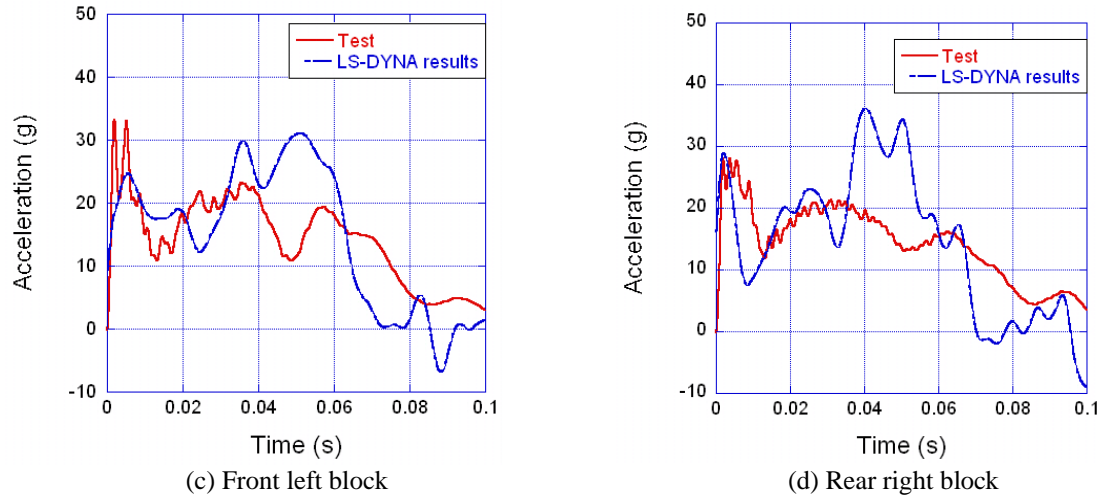(a) Center left block

(b) Center right block

(c) Front left block   (d) Rear right block

Figure 11. Test/analysis correlation from different locations on the fuselage with DEA components impacting concrete.

Vertical Impact into Sand

Impact of the fuselage section, fitted with the DEA, into sand was also analyzed using the *MAT_24 material model to represent the DEA components. An image of the finite element model is shown in Figure 12. Like the rigid impact model, the fuselage orientation for sand impact was assumed to be perfectly vertical. The model contains 14 parts; 220,305 nodes and 229,582 elements including 129,736 Belytschko-Tsay quadrilateral shell elements, 99,618 hexagonal solid elements, 188 beam elements, and 40 concentrated mass elements. All material models and element configurations prescribed for all parts in the fuselage section used for rigid impact were applied here. The sand, which served as the impact surface in this simulation, was modeled using *MAT_SOIL_AND_FOAM. Information on the characterization of the sand used in this model can be found in Reference 9. A Kevlar sheet, also modeled using *MAT_24, was placed beneath all DEA components to prevent the honeycomb from shearing through the sand (a "cookie cutter" effect) and thus effectively transferring the impact loads to each of the cell walls. Tied contacts were prescribed between the Kevlar sheet and the DEA components, and the bottom of the fuselage and the DEA components through the *TIED_SHELL_EDGE_TO_SURFACE option in LS-DYNA. The *CONTACT_AUTOMATIC_SINGLE_SURFACE algorithm was used to define contact between the sand and the DEA and self-contact within each component. An impact velocity of 37.4 fps was prescribed to the fuselage section with the DEA components. In this simulation, the crater depths in the sand ranged between 9 and 10.5 inches, and the crush of each DEA component ranged between 5 and 8 inches. In the test, between 7.5 and 9 inches of penetration into the sand was observed, and the amount of crush in the DEA was measured to about the same range as the penetration [9]. Acceleration response comparisons of four different lead block locations on the floor of the fuselage can be observed in Figure 13. The general analysis trends show good correlation with the test. All acceleration results were filtered at 60 Hz using an SAE low-pass filter.
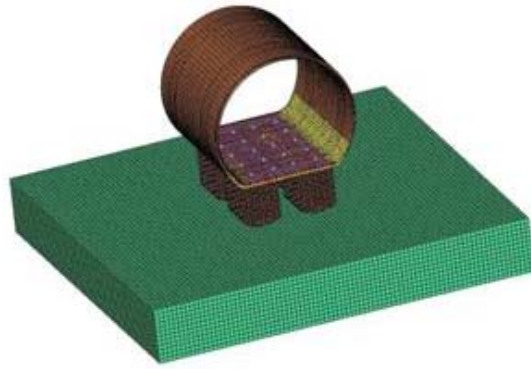
13

Figure 12. Picture of Composite Fuselage model with DEA components and sand
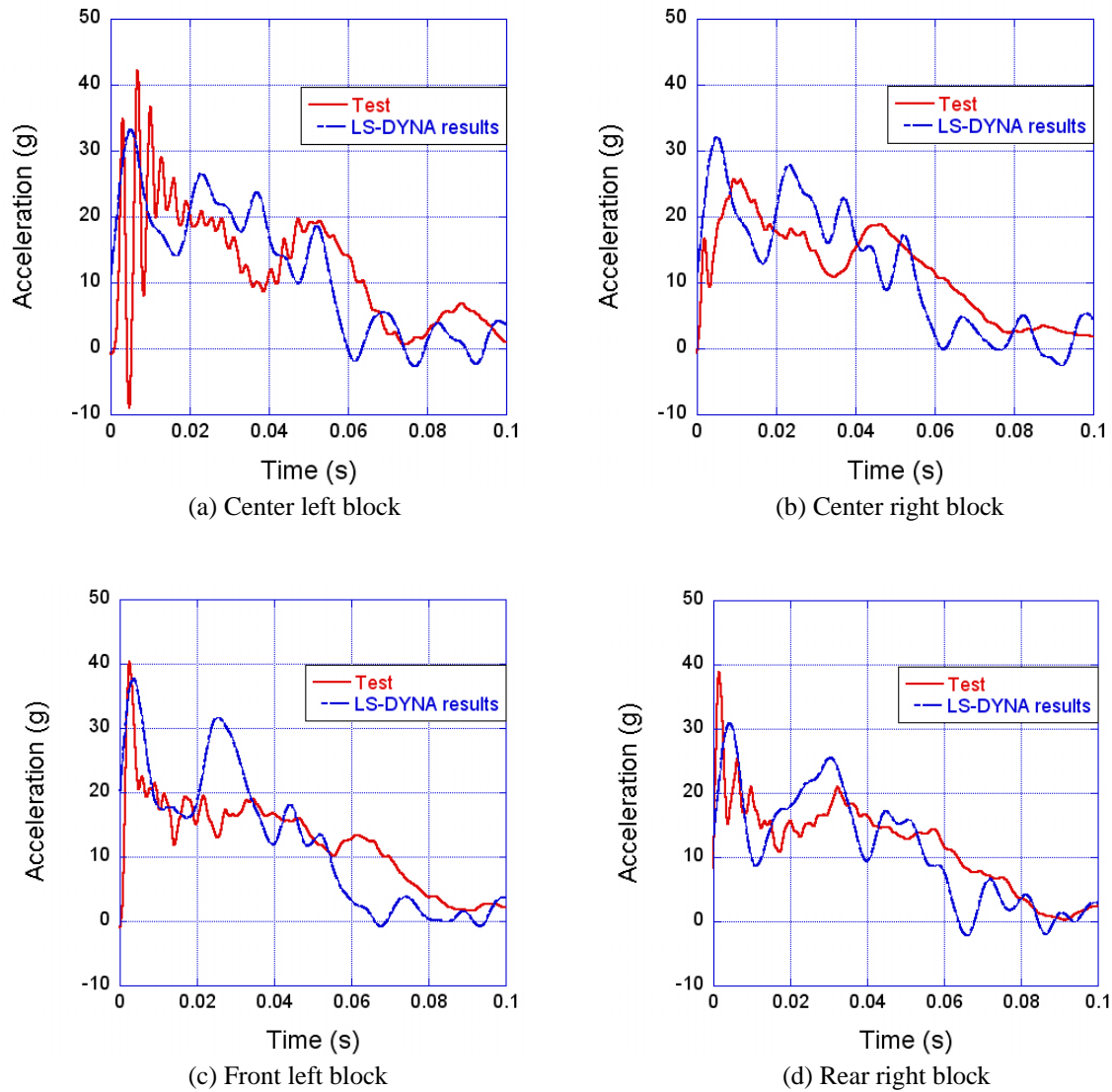

(a) Center left block

(b) Center right block

(c) Front left block

(d) Rear right block

Figure 13. Test/analysis correlation from different locations on the fuselage with DEA components impacting sand.

Discussion of Results

The simultaneous interaction of loading mechanisms in tension, compression, and shear within the Kevlar/Epoxy cell walls make it difficult to characterize accurately. As seen from three-point bend test/analysis correlation, which employed the three modes, the elastic and shear property values defined in *MAT_58 needed to be precise enough to match closely with test data. The load-displacement behavior of the single-cells was captured and represented better here than the approach presented in Reference 1, where *MAT_58 was used in both cases. The load-displacement response was not captured within *MAT_24 since the material was generated by inputting the ±45° tensile coupon response directly. However, when the crushing responses of single DEA components are simulated, *MAT_24 does better at predicting the impact response than *MAT_58 due to its ability to capture most of the post-buckling behavior seen in the test. The *MAT_24 material model, in comparison with the *MAT_CRUSHABLE_FOAM material model used in Reference 1 to model the DEA, also does slightly better at predicting the impact response of the DEA with the fuselage section. The LS-DYNA acceleration plots for impact onto concrete show values higher than noted in the test acceleration curves after 0.02 seconds. An acceleration peak in the front left block of the fuselage during impact onto sand is also visible at about 0.025 seconds. This behavior is attributed to sudden collapse of elements within the DEA components. Overall, the impact behavior of the DEA into soft soil was well-predicted.

The *MAT_24 model in LS-DYNA takes into account the fiber scissoring that occurs when the cell walls react under a given load in tension through input of a stress-strain curve for the Kevlar/Epoxy composite. *MAT_58 does not account for fiber scissoring in its material model, and instead relies on the SLIM factors and material strengths to characterize deformation behavior in the composite at high strains. The SLIM factors play an important role in modeling composites using *MAT_58. For example, different crush responses of the 59-cell DEA component are shown in Figure 14 when the SLIM values are varied. All five SLIM parameters in *MAT_58 were set to 0.1 during this run (denoted in blue) and results are compared here to the property values specified in Table 2 (denoted in green). Lowering the stress-limited factors improves the sustained crush response of the DEA as shown in Figure 14.
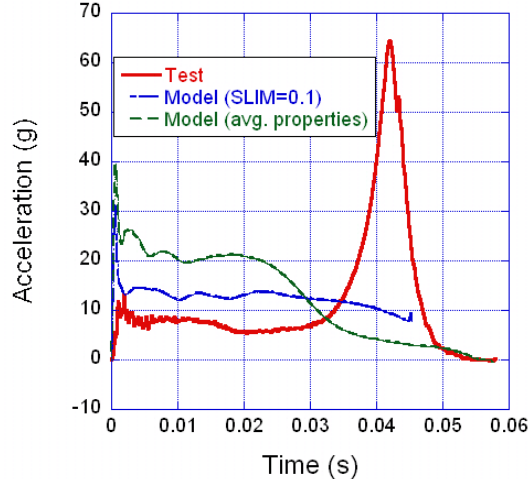

Figure 14. Effects of SLIM factors on 59-cell DEA crush response

The ERODS parameter in *MAT_58 has been utilized to simulate damage of composites in the past [5]. For the studies presented here, the ERODS parameter was set high since the Kevlar/Epoxy composite fails at very high strains, and the deletion of elements from the model led to distortion of neighboring elements responsible for driving down the time step. In addition, the strength values in tension, compression, and shear are important in characterizing the Kevlar/Epoxy composite. The behavior of the material after it "fails" is determined by the ultimate strength specified in tension, compression, and shear, in addition to the SLIM factors. Too high a strength value could lead to stiffening of the honeycomb, while a low strength value could lead to under-prediction of the crush response. While *MAT_24 performed well in predicting the crush response of the DEA, one must use caution when

15

defining an orthotropic material as isotropic in a finite element model. Nothing was certain about the behavior of the Kevlar/Epoxy composite other than the stress-strain behavior obtained from testing different composite fiber orientations in tension, which was the reason behind using an isotropic material model with a direct stress-strain input to define the DEA. This material model did well in predicting compressive behavior, but may not predict every load application that may exist for the DEA.

Conclusion

Two LS-DYNA material models were used to predict the material behavior of the Kevlar/Epoxy composite Deployable Energy Absorber (DEA) concept. A damage mechanics (*MAT_58) material model was used to predict the response of the Kevlar/Epoxy cell walls under three-point bending and dynamic crushing of the DEA. Using property values obtained from Response Surface Methodology and then averaged, the *MAT_58 material model closely predicted the three-point bend response of single hexagonal cells, but significantly over-predicted the DEA component crush response. As a result, the deformation modes seen from the test were not captured. In contrast, an elastic-plastic material model (*MAT_24) was used, which input the stress-strain response of the Kevlar/Epoxy composite having a ±45° orientation, to predict the material response of the DEA. The impact response of a fuselage section fitted with a system of DEAs was well predicted for simulations involving impact into sand and concrete. However, the load-displacement response of a single-cell under three-point bending was under-predicted and led to early failure.

References

[1] Kellas, S. and Jackson, K.E., "Deployable System for Crash-Load Attenuation." 63rd Annual AHS Forum, Virginia Beach, VA, May 1-3, 2007.
[2] Kellas, S., "Deployable Rigid System for Crash Energy Management," US Patent Nos. 6,755,453 on June 29, 2004; 6,976,729 on December 20, 2005; and 7,040,658 on May 9, 2006.
[3] Anon, "LS-DYNA Keyword User's Manual," Version 971, Livermore Software Technology Company, Livermore, CA, August 2006.
[4] Fleming, David C. "Modeling Composite Laminate Crushing for Crash Analysis." NAG-1-2260, 2001.
[5] Fasanella, E.L. and Kellas, S., "Quasi-Static 3-Point Reinforced Carbon-Carbon Bend Test and Analysis for Shuttle Orbiter Wing Leading Edge Impact Damage Thresholds." NASA/ 2006-214505, 2006.
[6] Matzenmiller, A., Lubliner, J., and Taylor, R.L., "A Constitutive Model for Anisotropic Damage in Fiber Composites, Mech. Mater, 1995; 20, 125-152.
[7] Horta, L., Jackson, K.E., and Kellas, S., "A Computational Approach for Model Update of an LS-DYNA Energy Absorbing Cell." Proceedings of the 64th American Helicopter Society Annual Forum, Montreal, Quebec, Canada, April 29-May 1, 2008.
[8] Kellas, S. and Jackson, K.E., "Multi-Terrain Vertical Drop Tests of a Composite Fuselage Section." Proceedings of the 64th American Helicopter Society Annual Forum, Montreal, Quebec, Canada, April 29-May 1, 2008.
[9] Fasanella, E.L. "Soft Soil Impact Testing and Simulation of Aerospace Structures." Proceedings of the 2008 LS-DYNA Conference, Dearborn, MI, 2008.